

# Transient state kinetic evidence for an oligomer in the mechanism of Na<sup>+</sup>–H<sup>+</sup> exchange

(Na<sup>+</sup> translocation/renal brush border membranes/amiloride/conformational transition/hormonal regulation)

KINYA OTSU\*, JAMES KINSELLA, BERTRAM SACKTOR, AND JEFFREY P. FROELICH

Laboratory of Biological Chemistry, National Institute on Aging, National Institutes of Health, Gerontology Research Center, 4940 Eastern Avenue, Baltimore, MD 21224

Communicated by Joseph F. Hoffman, March 13, 1989 (received for review July 6, 1988)

**ABSTRACT** Pre-steady-state kinetic measurements of <sup>22</sup>Na<sup>+</sup> uptake by the amiloride-sensitive Na<sup>+</sup>–H<sup>+</sup> exchanger in renal brush border membrane vesicles (BBMV) were performed at 0°C to characterize the intermediate reactions of the exchange cycle. At 1 mM Na<sup>+</sup>, the initial time course of Na<sup>+</sup> uptake was resolved into three separate components: (i) a lag phase, (ii) an exponential or “burst” phase, and (iii) a constant velocity or steady-state phase. Pulse–chase experiments using partially loaded BBMV showed no evidence for <sup>22</sup>Na<sup>+</sup> back-flux, suggesting that the decline in the rate of Na<sup>+</sup> uptake rate following the burst represents completion of the first turnover of the exchanger. Gramicidin completely abolished Na<sup>+</sup> uptake, indicating that the burst phase results from the translocation of Na<sup>+</sup> rather than from residual Na<sup>+</sup> binding to external sites. Raising the [Na<sup>+</sup>] from 1 to 10 mM at constant pH (internal pH 5.7; external pH 7.7) produced a sigmoidal increase in the amplitude of the burst phase without affecting the lag duration or the apparent burst rate. In contrast, Na<sup>+</sup> uptake in the steady state obeyed Michaelis–Menten kinetics. These results suggest that a minimum of two Na<sup>+</sup> transport sites must be occupied to activate Na<sup>+</sup> uptake in the pre-steady state. The transition to Michaelis–Menten kinetics in the steady state can be explained by a “flip-flop” or alternating site mechanism in which the functional transport unit is an oligomer and only one protomer per cycle is allowed to form a translocation complex with Na<sup>+</sup> after the first turnover.

The regulation of intracellular pH in the kidney proximal tubule is mediated by a Na<sup>+</sup>–H<sup>+</sup> exchange protein localized to the brush border membrane (1). Kinetic investigations performed under steady-state conditions have shown that the exchanger has a single transport site for Na<sup>+</sup> and at least two sites for H<sup>+</sup>, one of which has a regulatory function (2, 3). In addition to intrinsic regulation by protons, Na<sup>+</sup>–H<sup>+</sup> exchange activity is also subject to control by various extrinsic substances including hormones, growth factor, and pharmacologic agents (4, 5).

Although fairly detailed transport models depicting the sequence of ligand interactions with the Na<sup>+</sup>–H<sup>+</sup> exchanger have been proposed (1), the nature and sequence of events comprising the intermediate steps of the reaction mechanism are poorly understood. In the present study, we attempted to identify these reactions and to quantitate their kinetic behavior by measuring the pre-steady-state time course of H<sup>+</sup>-dependent Na<sup>+</sup> uptake in brush border membrane vesicles (BBMV) isolated from rabbit kidney cortex. A technical limitation involved minimizing the time of incubation between the addition of the substrate and the quench reagent so that the first turnover of the exchanger could be resolved. This was accomplished by lowering the incubation temperature to slow the reaction rate, thereby allowing the mixing

operations to be carried out by hand with the aid of a metronome. The reaction was rapidly terminated by dilution of the vesicles into a medium containing amiloride, which prevented further <sup>22</sup>Na<sup>+</sup> uptake as well as <sup>22</sup>Na<sup>+</sup> efflux.

We report here that amiloride-sensitive Na<sup>+</sup> uptake in H<sup>+</sup>-loaded BBMV exhibits a rapid phase of accumulation that is sensitive to gramicidin. Analysis of the data suggests that this behavior reflects the initial turnover of the exchanger, implying that Na<sup>+</sup> translocation is not rate-limiting at 0°C.

## MATERIALS AND METHODS

**Preparation of BBMV.** BBMV, predominantly in the right-side out configuration, were isolated from rabbit kidney cortex as described (6) and used immediately following preparation. Protein concentration was determined by the method of Lowry *et al.* (7) with bovine serum albumin as standard.

**<sup>22</sup>Na<sup>+</sup> Uptake Assay.** Prior to measuring Na<sup>+</sup> uptake, the vesicles were suspended in 150 mM KCl and 10 mM Tris/16 mM Hepes adjusted with Mes [2-(*N*-morpholino)ethanesulfonic acid] to the final desired pH values and then incubated at 20°C for 90 min to allow the ligands in the intra- and extravascular spaces to equilibrate. For the determination of Na<sup>+</sup> uptake at 0°C, 25 μl of membrane suspension (250–500 μg of protein) was deposited on the bottom of a 13 × 100 mm glass test tube placed inside a sealed 17 × 90 mm clear polystyrene tube containing 2 ml of ice-cold water. The outer tube served as an insulator for maintaining the reaction temperature at 0°C. On the wall above the membrane suspension, 25 μl of the incubation medium containing <sup>22</sup>Na<sup>+</sup> (0.1–0.2 μCi; 1 Ci = 37 GBq) was added to the tube. A dried film of bovine serum albumin on the inner surface of the glass tube prevented solutions from running down the side and mixing with the membrane suspension. The tubes were returned to the ice for at least 2 min prior to starting the reaction. Incubations were initiated by shaking the tubes with a Vortex mixer and a metronome was used to time the duration of Na<sup>+</sup> uptake. Incubations were terminated by the manual addition of 3 ml of an ice-cold quench solution containing 100 μM amiloride hydrochloride, 150 mM KCl, and 10 mM Tris/16 mM Hepes, pH 7.5. The membranes were harvested on a 0.65-μm pore size filter and rinsed with an additional 9 ml of the quench solution to remove nonspecifically bound isotope. The 60:1 dilution of the reaction mixture by the quench solution containing 100 μM amiloride was found to prevent further <sup>22</sup>Na<sup>+</sup> uptake and to block <sup>22</sup>Na<sup>+</sup> efflux from BBMV. In the absence of Na<sup>+</sup>-dependent trans-

The publication costs of this article were defrayed in part by page charge payment. This article must therefore be hereby marked “advertisement” in accordance with 18 U.S.C. §1734 solely to indicate this fact.

Abbreviation: BBMV, brush border membrane vesicle(s).

\*To whom reprint requests should be addressed at: Charles H. Best Institute, University of Toronto, 112 College Street, Toronto, ON M5G1L6, Canada.

portable organic solutes, amiloride-sensitive  $\text{Na}^+$  uptake occurs exclusively through the  $\text{Na}^+-\text{H}^+$  exchanger.

**Kinetic Modeling.** Computer simulations of time-dependent  $\text{Na}^+$  accumulation were carried out using the curve-fitting routines contained in MLAB (modeling laboratory) (8). Biomolecular reactions were simulated by using the pseudo-first-order approximation and the assumption that extravesicular  $\text{Na}^+$  binding involves a rapid equilibrium with a weak ( $K_D = 0.005 \text{ M}$ ) binding site. The remaining initial conditions for the simulations (e.g., transport site density, first-order rate constants) were estimates derived from the time-dependent  $\text{Na}^+$  uptake data by standard graphical procedures. Optimization of the computer-generated fits were accomplished by means of a least-squares curve-fitting routine (8) or simply by eye.

## RESULTS AND DISCUSSION

At  $20^\circ\text{C}$ ,  $\text{H}^+$ -dependent  $^{22}\text{Na}^+$  uptake by the  $\text{Na}^+-\text{H}^+$  exchanger in BBMV follows a linear time course that extrapolates through the origin at  $t = 0$  (9). Lowering the reaction temperature to  $0^\circ\text{C}$  produced several distinct changes in the qualitative and the quantitative behavior of the  $\text{Na}^+$  uptake time course as shown in Fig. 1A. Between 0.5 and 2 s, a rapid initial phase or burst of  $^{22}\text{Na}^+$  uptake was observed followed by a linear (constant velocity) phase that lasted several seconds. When this experiment was repeated in the presence of 1 mM amiloride,  $\text{Na}^+$  was taken up more slowly and followed a linear time course (Fig. 1A, lower curve). These results demonstrate that a major portion of the  $\text{Na}^+$  uptake measured during the rapid phase of accumulation at  $0^\circ\text{C}$  in the absence of inhibitor is due to the activity of the amiloride-sensitive  $\text{Na}^+-\text{H}^+$  exchanger.

The curve remaining after subtraction of amiloride-insensitive  $^{22}\text{Na}^+$  uptake from the transport activity measured in the absence of amiloride was used to evaluate the kinetic parameters of  $\text{H}^+$ -dependent  $\text{Na}^+$  accumulation. At 1 mM  $\text{Na}^+$ , the size of the burst or burst amplitude, determined by extrapolation of the linear phase of amiloride-sensitive  $\text{Na}^+$  uptake to  $t = 0$ , was 0.155 nmol of  $\text{Na}^+$  per mg of protein. This value approximates the concentration of actively transporting sites, assuming that the burst phase represents the first turnover of the exchanger. A semilogarithmic plot of the difference between the extrapolated steady state and each of

the preceding time points (Fig. 1A *Inset*) gave a straight line with a slope of  $0.74 \text{ s}^{-1}$ , corresponding to the apparent burst rate. The initial downward deflection in the semilogarithmic plot, which can be seen more clearly in the experiments shown in Fig. 1B, is due to the presence of an early lag in  $\text{Na}^+$  uptake that precedes the formation of the burst phase. Although the lag phase varied somewhat between preparations, it was not affected by changing the  $\text{Na}^+$  concentration within a given preparation (Fig. 1B). This implies that the initial delay in  $\text{Na}^+$  uptake is not caused by the formation of a collision complex between  $\text{Na}^+$  and the transport site, but it is probably due to the presence of a slow first-order transition that precedes  $\text{Na}^+$  binding and/or translocation.

The exponential behavior of the transient phase of  $\text{Na}^+$  accumulation and the linear time dependence of  $\text{Na}^+$  uptake that occurs subsequently suggests that the burst corresponds to the initial turnover of the exchanger. An alternative possibility is that the decline in rate of  $\text{Na}^+$  uptake after 2 s is due to  $^{22}\text{Na}^+$  backflux, which will increase as the vesicles become loaded with  $\text{Na}^+$ . To test whether significant  $^{22}\text{Na}^+$  backflux occurs under these conditions, the vesicles were partially loaded with  $^{22}\text{Na}^+$  and then chased with a pulse of  $^{23}\text{Na}^+$  while maintaining a constant level of  $\text{Na}^+$  in the incubation medium. No amiloride-sensitive efflux of labeled  $\text{Na}^+$  was detected over a 10-s time interval when the cold chase was added to vesicles that contained an amount of  $\text{Na}^+$  that was either less than (0.1 nmol/mg) or greater than (0.5 nmol/mg) the amount accumulated during the burst phase. Incubating the vesicles with gramicidin (400  $\mu\text{g}$  in 3% dimethyl sulfoxide per mg of protein) for 90 min at  $20^\circ\text{C}$  prior to measuring the exchange activity completely eliminated  $\text{Na}^+$  uptake at  $0^\circ\text{C}$  (data not shown). This suggests that  $\text{Na}^+$  accumulated during the burst phase is internalized since the ionophore should have only released  $\text{Na}^+$  trapped inside the vesicle without affecting membrane-bound  $\text{Na}^+$ .

As shown in Table 1, the burst amplitude and the steady-state velocity were dependent on the internal  $\text{H}^+$  concentration. At 1 mM  $\text{Na}^+$ , decreasing the internal pH from 7.17 to 6.0 produced a 3-fold increase in the burst amplitude without affecting the apparent burst rate. The apparent turnover number, obtained by dividing the steady-state velocity by the burst amplitude, almost doubled over this pH range, consistent with the observation that the  $\text{Na}^+-\text{H}^+$  exchanger con-

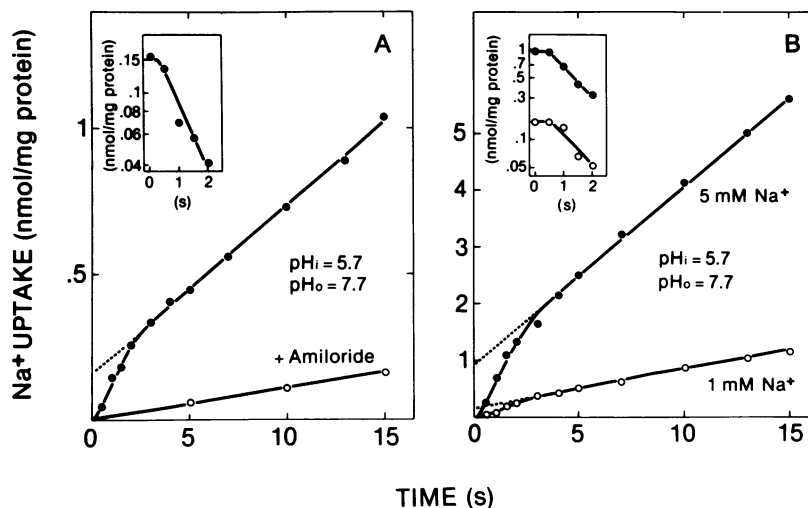


FIG. 1. Time dependence of  $^{22}\text{Na}^+$  uptake by BBMV at  $0^\circ\text{C}$ . (A) Time course of total (amiloride sensitive plus amiloride insensitive)  $^{22}\text{Na}^+$  uptake ( $\bullet$ ) at 1 mM  $\text{Na}^+$ . Amiloride-insensitive  $^{22}\text{Na}^+$  uptake ( $\circ$ ) was measured by including 1 mM amiloride in the incubation medium. (B) Amiloride-insensitive  $^{22}\text{Na}^+$  uptake was subtracted from the total  $^{22}\text{Na}^+$  uptake at 1 mM ( $\circ$ ) and 5 mM ( $\bullet$ )  $\text{Na}^+$  prior to plotting the data. (*Insets*) Semilogarithmic plots of  $\text{Na}^+$  uptake during the burst phase obtained by subtracting the pre-steady-state time points from the extrapolated steady state and plotting the difference as a function of the incubation time.

Table 1. Kinetic constants for amiloride-sensitive  $^{22}\text{Na}^+$  uptake in BBMV at  $0^\circ\text{C}$ 

$\text{pH}_i$	$[\text{Na}]_o$ , mM	Burst amplitude,* nmol/mg	Rate constant, <sup>†</sup> $\text{s}^{-1}$	Steady-state velocity, <sup>‡</sup> $\text{nmol}\cdot\text{mg}^{-1}\cdot\text{s}^{-1}$	Turnover number, <sup>‡</sup> $\text{s}^{-1}$
6.0	1.0	$0.166 \pm 0.014$	0.730	$0.038 \pm 0.0059$	0.231
7.17	1.0	$0.0515 \pm 0.0059$	0.750	$0.00694 \pm 0.0007$	0.134
5.7	1.0	$0.118 \pm 0.010$	0.814	$0.0667 \pm 0.0078$	0.565
5.7	5.0	$0.625 \pm 0.055$	0.825	$0.200 \pm 0.032$	0.320

Measurements of the time course of amiloride-sensitive  $^{22}\text{Na}^+$  uptake by the  $\text{Na}^+-\text{H}^+$  exchanger were performed at  $0^\circ\text{C}$ . The intravesicular pH ( $\text{pH}_i$ ) was adjusted to the value shown by incubation in the appropriate buffer and the final external pH was adjusted to 7.7 by dilution of the vesicles into a medium containing  $^{22}\text{Na}^+$  at the concentrations indicated. Values are expressed as means  $\pm$  SEM of at least three different membrane preparations.

\*The burst amplitude was determined by extrapolation of the linear or steady-state phase of  $\text{Na}^+$  uptake to  $t = 0$ .

<sup>†</sup>The apparent burst rate was evaluated from the slope of the semilogarithmic plot of the burst phase of  $\text{Na}^+$  uptake.

<sup>‡</sup>The apparent turnover number was calculated from the steady-state velocity of  $\text{Na}^+$  uptake divided by the burst amplitude.

tains an internal  $\text{H}^+$ -dependent regulatory site that activates  $\text{Na}^+$  uptake at acidic pH (3).

Fig. 1B compares the time courses of amiloride-sensitive  $^{22}\text{Na}^+$  uptake in  $\text{H}^+$ -loaded BBMV at 1 mM and 5 mM  $\text{Na}^+$ . The curves are qualitatively identical and show similar quantitative characteristics with respect to both the lag duration and apparent burst rate (see also Table 1). However, quantitative differences were found in the burst amplitude and the steady-state velocity, which differed by factors of 5 and 3, respectively. This result was unexpected since it suggests that the pre-steady-state burst and the overall velocity become saturated at different  $\text{Na}^+$  levels. This was explored in greater detail by examining  $\text{Na}^+$  accumulation in the burst phase and steady state over a 10-fold  $\text{Na}^+$  concentration range (1–10 mM). As shown in Fig. 2A, the relationship between the burst amplitude and  $\text{Na}^+$  concentration was sigmoidal with a half-maximal saturation occurring at  $\approx 4$  mM  $\text{Na}^+$  and a plateau between 7 and 10 mM  $\text{Na}^+$ . In contrast, the  $[\text{Na}^+]$  dependence of the steady-state velocity obeyed Michaelis-Menten kinetics (Fig. 2B) with a  $K_m$  of  $\approx 6$  mM, similar to the behavior found at  $20^\circ\text{C}$  (2, 4).

The possibility that different subpopulations of the vesicles contribute to the multiphasic time course of  $\text{Na}^+$  uptake is inconsistent with the observation that the burst amplitude is a saturable function of the  $\text{Na}^+$  concentration (Fig. 2A). Had the transient phase of  $\text{Na}^+$  uptake resulted from equilibration of  $\text{Na}^+$  transport in a rapidly filling population of vesicles,

then the amount of  $\text{Na}^+$  taken up should have increased linearly with  $[\text{Na}^+]$  rather than approaching saturation. In addition, the onset of equilibration should have been prolonged at higher  $\text{Na}^+$  concentrations, causing the apparent burst rate to decline rather than remain independent of the  $[\text{Na}^+]$ . Another phenomenon producing burst kinetics is hysteresis, which results from having two different conformational states of the exchange protein with different  $\text{Na}^+$  binding affinities and catalytic activities (10). In this case, the rate of transition to the less active conformation depends on the  $\text{Na}^+$  concentration, becoming faster as the  $[\text{Na}^+]$  is raised. Because we observed no change in the apparent burst rate in response to changing the  $[\text{Na}^+]$ , we conclude that hysteresis is probably not responsible for the complex time dependence of  $\text{Na}^+$  uptake in Fig. 1. Further support for this conclusion comes from experiments conducted at low (0.1–1 mM)  $\text{Na}^+$  concentrations (data not shown), which gave an apparent burst rate similar to that measured at higher  $\text{Na}^+$  levels (0.6–0.8  $\text{s}^{-1}$ ).

The above considerations support the conclusion that the rapid phase of  $\text{Na}^+$  uptake at  $0^\circ\text{C}$  corresponds to the inward movement of  $\text{Na}^+$  across the brush border membrane coupled to the initial cycle of  $\text{Na}^+-\text{H}^+$  exchange. Raising the incubation temperature to  $20^\circ\text{C}$  converts the time course of  $\text{Na}^+$  uptake to linear kinetics (2), indicating that the exchange mechanism includes a reaction with an activation energy exceeding that of  $\text{Na}^+$  translocation that becomes rate-limiting at reduced temperatures. Assuming that the bound and free ligands are in rapid equilibrium, plausible candidates for the rate-limiting step at  $0^\circ\text{C}$  include recycling of the  $\text{H}^+$ -loaded carrier or a slow conformational transition following  $\text{Na}^+$  translocation. A specific example of the latter alternative, suggested by studies on the mechanism of  $\text{Na}^+-\text{Ca}^{2+}$  exchange (11, 12), is a change in protein conformation involving the conversion of a  $\text{Na}^+$ -specific binding conformation ( $C_o$ ) to a  $\text{H}^+$ -specific form ( $C_i$ ) as shown below (step 6):

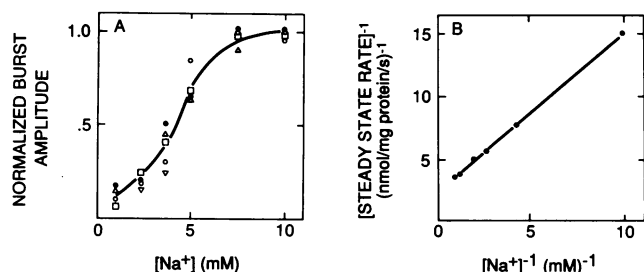
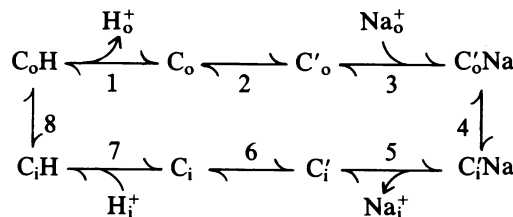


FIG. 2. Sodium ion concentration dependence of the burst and steady-state phases of amiloride-sensitive  $\text{Na}^+$  uptake. Standard incubation conditions were used for measuring  $^{22}\text{Na}^+$  uptake by the amiloride quench technique. The burst amplitude was evaluated at each  $\text{Na}^+$  concentration by extrapolation of the steady-state portion of the uptake curve to  $t = 0$ . (A) The plot of burst amplitude vs.  $[\text{Na}^+]$  was constructed from five separate experiments after normalizing each data set to the maximum burst amplitude to correct for differences in transport activity. (B) Double reciprocal plot of the average steady-state  $\text{Na}^+$  uptake velocity (evaluated from the same set of five experiments) vs.  $[\text{Na}^+]$ .



where the subscripts i and o refer to inwardly and outwardly facing orientations of the carrier, respectively. According to this model, there are four conformational transformations in

the exchange cycle, two of which are directly involved in ion translocation. The initial conditions of the transport assay favor accumulation of the carrier in the two  $H^+$ -loaded states in the left-hand portion of the cycle since both sides of the membrane were acidic (pH 5.7) prior to the addition of  $Na^+$ . Upon dilution into the alkaline  $^{22}Na^+$ -containing medium, a  $H^+$  is released from the carrier externally generating  $C_o$  (step 1). To bind and transport  $Na^+$ , the carrier must first undergo a change in conformation from  $C_o$  to  $C'_o$  (step 2), which may be responsible for the lag phase. This step may also control the kinetics of the burst phase if it is slow compared to  $Na^+$  binding (step 3) and translocation (step 4) that occur immediately afterwards. Following  $Na^+$  dissociation at the inner membrane surface (step 5), the carrier proceeds through the reverse transformation,  $C'_i$  to  $C_i$ , converting it back to a form that preferentially binds  $H^+$ . To account for the presence of the burst phase, this reaction should take place at a slower rate than the forward transition at step 2, assuming that  $H^+$  translocation (step 8) is fast. Alternatively, rate-limitation might result from the slow release of  $Na^+$  internally or from  $H^+$  translocation (step 8) being slower than  $Na^+$  translocation. In the former case, the kinetics of the dissociation reaction would presumably reflect the release of  $Na^+$  from an occluded state, since the low affinity of the exchanger for  $Na^+$  implies that this ligand comes on and off the carrier at fairly high rates.

Resolution of the initial turnover of the exchanger at  $0^\circ C$  enabled us to estimate the transport site density from the amplitude of the burst phase. At saturating  $Na^+$ , the burst amplitude was  $\approx 1$  nmol/mg, which is considerably larger than the site densities reported in lymphocytes (13) and solubilized renal BBMV (14). In the latter study, the lower site density (2 pmol/mg) may reflect a loss of transporters due to denaturation and/or incomplete recovery following exposure to the detergent and prior to covalent labeling with the amiloride analog. Our results suggest that the  $Na^+-H^+$  exchanger is a major component of the brush border membrane, which is not surprising in view of the large amount of  $Na^+$  that must be reabsorbed from the glomerular filtrate to maintain cellular electrolyte balance. In a recent study, Sardet *et al.* (15) using a genetic approach reported a molecular mass of the human  $Na^+-H^+$  exchanger of 99 kDa, while Karpel *et al.* (16) obtained a value of 35 kDa for the exchange protein in *Escherichia coli*. At a transport site density of 1 nmol per mg of BBMV protein, the  $Na^+-H^+$  exchanger would comprise between 3% and 10% of the total membrane protein assuming that its molecular mass is in the 30- to 100-kDa range. In agreement with this prediction, SDS/polyacrylamide gels stained with Coomassie blue (17, 18) show several intense protein bands that fall within this size range. While these results lend support to our interpretation of the burst phenomenon, a definitive answer to this question awaits identification of the BBMV exchange protein, and the most compelling evidence for the initial turnover is the lack of an alternative explanation that is fully consistent with the pre-steady-state kinetic behavior.

Although  $Na^+$  accumulation in the steady state obeys Michaelis-Menten kinetics (Fig. 2B), the sigmoidal relationship between the burst amplitude and  $[Na^+]$  in Fig. 2A suggests a more complex interaction involving multiple  $Na^+$  binding sites. This interpretation should be viewed with caution since the quantity measured by extrapolation of the steady state to  $t = 0$  (or burst amplitude) is not equivalent to the steady-state concentration of the transport intermediate that accumulates during the burst phase. The latter variable (like the steady-state velocity) will show a dependence on  $Na^+$  that reflects both the number of  $Na^+$  binding sites involved and the way in which those sites interact as they become occupied (19). The burst amplitude, on the other hand, may show a sigmoidal response to  $Na^+$  even when only one site is available to bind  $Na^+$  (20, 21). To evaluate the  $Na^+$  dependence of the exchange reaction in the pre-steady state, we resorted to computer

simulation of the burst phase intermediate by using a simplified version of the previous transport mechanism. This is shown in Fig. 3 for the data at 5 mM  $Na^+$ , which is replotted from Fig. 1B. The time points are closely approximated by a curve representing the sum of the time course of formation of the burst phase intermediate plus  $Na^+$  uptake after the first turnover. After a brief lag, the intermediate increases by an exponential time course to a final or steady-state level given by  $C_s$ . It can be seen that the burst amplitude,  $B_o$ , underestimates  $C_s$  and that they begin to approach each other as the steady-state rate becomes smaller (for a single turnover,  $C_s = B_o$ ). We find that as the  $Na^+$  concentration is raised (1 mM to 5 mM),  $Na^+$  uptake in the steady state declines relative to that in the burst phase because of a decrease in the apparent turnover number (0.5 to 0.3; Table 1). Thus, the ratio of  $B_o$  to  $C_s$  does not remain constant but is an increasing function of  $[Na^+]$ . To

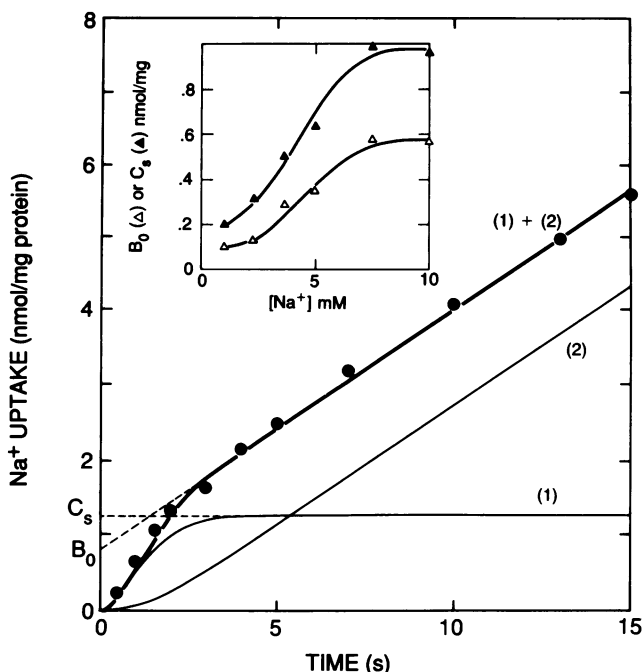
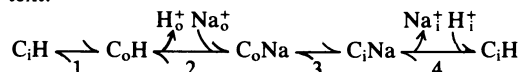


FIG. 3. Simulation of the burst-phase intermediate and  $Na^+$  dependence of its steady-state level of formation. The time dependence of formation of the intermediate corresponding to the burst phase was simulated by using a simplified version of the model given in the text:



The best fit of the model to the experimental data at 5 mM  $Na^+$  (●) was obtained by using a site density of 1.87 nmol/mg and the following set of values for the forward ( $k_i$ ) and reverse ( $k_{-i}$ ) rate constants (in  $s^{-1}$ ):  $k_1/k_{-1} = 0.8/0$ ;  $k_2[Na]/k_{-2} = 5 \times 10^3/5 \times 10^3$ ;  $k_3/k_{-3} = 10/0$ ;  $k_4/k_{-4} = 0.25/0$ . Initial conditions for the simulation were chosen so that  $[C_iH] = 1.87$  nmol/mg and all other intermediate concentrations were zero. The simulated time course of  $Na^+$  uptake (optimization by eye), represented by the heavy curve, equals the sum of (i) the time course of formation of the burst-phase intermediate,  $C_iNa$ , and (ii) the time dependence of  $Na^+$  uptake after the first turnover. (Inset) The steady-state level of formation of the burst-phase intermediate,  $C_s$ , was evaluated for each set of data points at the different  $Na^+$  concentrations plotted on the abscissa. A least-squares curve-fitting routine (8) was used to optimize these simulations. The corresponding values for the burst amplitude,  $B_o$ , are shown for comparison. Simulation of  $Na^+$  accumulation using the single-site model required increasing the transport site concentration from 0.347 nmol/mg to 1.58 nmol/mg as the  $Na^+$  concentration was raised from 1 to 10 mM. Different preparations were used in the experiments shown in the figure and the Inset, accounting for the difference in transport activity.

determine how  $C_s$  varies with  $\text{Na}^+$ , the steady-state concentration of the burst phase intermediate was evaluated from the time course of  $\text{Na}^+$  uptake at each  $\text{Na}^+$  concentration as described above. It should be noted that the single-site mechanism used in these simulations (cf. legend to Fig. 3) was unable to reproduce the time course of  $\text{Na}^+$  uptake over the entire range of  $\text{Na}^+$  concentrations (1–10 mM) without increasing the transport site density along with the  $\text{Na}^+$  concentration. (The implication of this result is that a single-site mechanism is inadequate and that a more complex scheme involving at least two  $\text{Na}^+$  binding sites is needed to explain the  $\text{Na}^+$  concentration dependence of the pre-steady-state burst.) The steady-state intermediate levels ( $C_s$ ) are plotted in Fig. 3 (*Inset*) together with the corresponding values of  $B_0$  at each  $\text{Na}^+$  level. It is apparent that  $C_s$  shows the same qualitative response to  $\text{Na}^+$  as  $B_0$ —i.e., the plot of  $C_s$  vs.  $[\text{Na}^+]$  is sigmoidal. This is the predicted response for a system possessing multiple interacting sites, implying that activation of the exchange reaction involves a cooperative interaction between  $\text{Na}^+$  transport sites.

Alternatively, monomeric transport systems may exhibit cooperative kinetic behavior due to the presence of hysteresis or a random-order bisubstrate addition mechanism. The first of these was considered in relation to the burst mechanism and was eliminated on the grounds that the apparent burst rate did not vary with  $[\text{Na}^+]$ . Apparent cooperativity may also arise in a situation in which  $\text{Na}^+$  and  $\text{H}^+$  binding are both necessary for the activation of  $\text{Na}^+$  translocation and in which  $\text{Na}^+$  binding is kinetically favored, but random with respect to  $\text{H}^+$  binding. However, this behavior will only occur at subsaturating internal  $\text{H}^+$  concentrations, which were not used in the present study (internal pH 5.7).

A transport mechanism involving a single (monomeric) exchange protein could give rise to the complex  $\text{Na}^+$  dependence of the burst phase if the exchanger contained both regulatory and transport sites for  $\text{Na}^+$ . However, this seems unlikely in view of the fact that gramicidin completely eliminated  $\text{Na}^+$  accumulation, suggesting that the  $\text{Na}^+$  binding sites on the exchanger are exclusively involved in transport. A monomeric scheme involving two or more interactive  $\text{Na}^+$  transport sites is also a possibility, although in this case the positive cooperativity expressed in the burst phase would have to disappear after the first turnover to account for the simple (Michaelis–Menten)  $\text{Na}^+$  dependence in the steady state (Fig. 2B). A plausible solution to this problem is afforded by the “flip-flop” type of mechanism in which the functional transport unit is an oligomer and the subunits alternate their conformational and ligand binding properties during transport (22). In this scheme, the initial cycle of transport involves a unique set of events in which  $\text{Na}^+$  binds to a single site on each of the protomers comprising the oligomer and is then transported to the inside of the vesicle as shown in the upper pathway of Fig. 4 for the case of a dimer. To account for the positive cooperativity of the burst phase, the second  $\text{Na}^+$  has to bind more tightly than the first. In each subsequent exchange cycle,  $\text{Na}^+$  movement in one direction across the membrane is conformationally coupled to  $\text{H}^+$  translocation in the opposite direction on the adjacent subunit (Fig. 4, lower pathway) yielding the simple  $\text{Na}^+$  dependence observed in the steady state. A central feature of this model, which was originally proposed by Chappellet-Tordo *et al.* (23) to account for similar behavior in alkaline phosphatase and has been reported to exist in several other polymeric enzymes (22), is the transition from the complex  $\text{Na}^+$  dependence observed during the initial turnover of the exchanger to the simple  $\text{Na}^+$  dependence seen in subsequent turnovers. It should be noted that the mechanism requires occupation of adjacent  $\text{Na}^+$  binding sites during the initial transport cycle; otherwise there would not be an opportunity for a cooperative binding interaction in the pre-steady state. In support of this proposal, we

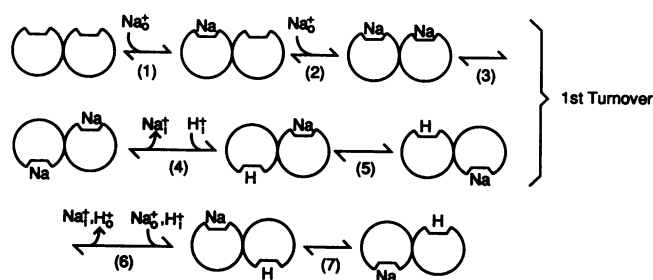


FIG. 4. Flip-flop mechanism for  $\text{Na}^+$ – $\text{H}^+$  exchange. The exchanger is a functional diprotomer with interconvertible binding sites for  $\text{Na}^+$  and  $\text{H}^+$ . The subscripts *i* and *o* refer to the intra- and extravesicular compartments, respectively. The final intermediate state in the second turnover of the exchanger (lower line) is equivalent to the final intermediate in the first turnover by a symmetrical transformation. Further details are provided in the text.

have recently observed that an inside-negative membrane potential enhances  $\text{Na}^+$  uptake during the initial transport cycle but has no effect on the steady-state activity (unpublished observation). This could have resulted from the accumulation of positive charge associated with the uncompensated movement of the  $\text{Na}^+$  to the inside of the vesicle during the initial turnover. In the subsequent cycles, the stoichiometric (electroneutral) exchange of internal  $\text{H}^+$  for external  $\text{Na}^+$  would prevent further charge accumulation and its effect on  $\text{Na}^+$  influx. Although these features of the exchange kinetics conform to the predictions of the flip-flop mechanism, further work is necessary to establish the molecular basis of this complex behavior.

We thank Mr. Phillip Heller for assistance in computer modeling the time dependence of  $\text{Na}^+$  accumulation by the  $\text{Na}^+$ – $\text{H}^+$  exchanger.

- Aronson, P. S. (1985) *Annu. Rev. Physiol.* **47**, 545–560.
- Kinsella, J. L. & Aronson, P. S. (1981) *Am. J. Physiol.* **241**, F374–F379.
- Aronson, P. S., Nee, J. & Suhm, M. A. (1982) *Nature (London)* **299**, 161–163.
- Grinstein, S. & Rothstein, A. (1986) *J. Membr. Biol.* **90**, 1–12.
- Kinsella, J. L., Cujdik, T. & Sacktor, B. (1984) *Proc. Natl. Acad. Sci. USA* **81**, 630–634.
- Aronson, P. S. (1978) *J. Membr. Biol.* **42**, 81–98.
- Lowry, O. H., Rosebrough, N. J., Farr, A. L. & Randall, R. J. (1951) *J. Biol. Chem.* **193**, 265–275.
- Knott, G. D. (1979) *Comput. Programs Biomed.* **10**, 271–280.
- Kinsella, J., Cujdik, T. & Sacktor, B. (1984) *J. Biol. Chem.* **259**, 13224–13227.
- Neet, K. E. & Ainslie, G. R., Jr. (1980) *Methods Enzymol.* **64**, 192–226.
- Sutko, J. L. & Reeves, J. P. (1983) *J. Biol. Chem.* **258**, 3178–3182.
- Blaustein, M. P. & Russell, J. M. (1975) *J. Membr. Biol.* **22**, 285–312.
- Dixon, J. S., Cohen, S., Cragoe, E. J., Jr., & Grinstein, S. (1987) *J. Biol. Chem.* **262**, 3626–3632.
- Vigne, P., Jean, T., Barbry, P., Frelin, C., Fine, L. G. & Lazdunski, M. (1985) *J. Biol. Chem.* **260**, 14120–14125.
- Sardet, C., Franchi, A. & Pouyssegur, J. (1989) *Cell* **56**, 271–280.
- Karpel, R., Olami, Y., Taglicht, D., Schuldiner, S. & Padan, E. (1988) *J. Biol. Chem.* **263**, 10408–10414.
- Hammerman, M. R., Hansen, V. A. & Morrissey, J. J. (1982) *J. Biol. Chem.* **259**, 12380–12386.
- Weinman, E. J., Shenolikar, S. & Kahn, A. M. (1987) *Am. J. Physiol.* **252**, F19–F25.
- Segel, I. H. (1975) *Enzyme Kinetics* (Wiley, New York), pp. 534–535.
- Ouellet, L. & Stewart, J. A. (1959) *Can. J. Chem.* **37**, 737–743.
- Gutfreund, H. (1977) *Enzymes: Physical Principles* (Wiley, London), pp. 199–201.
- Lazdunski, M. (1972) *Curr. Top. Cell. Regul.* **6**, 267–310.
- Chappellet-Tordo, D., Fosset, M., Iwatsubo, M., Gache, C. & Lazdunski, M. (1974) *Biochemistry* **13**, 1788–1795.